

Arabidopsis Putative Deacetylase AtSRT2 Regulates Basal Defense by Suppressing *PAD4*, *EDS5* and *SID2* Expression

Chunzheng Wang, Feng Gao, Jianguo Wu, Jianli Dai, Chunhong Wei and Yi Li*

National Laboratory of Protein Engineering and Plant Genetic Engineering, National Center for Plant Gene Research (Beijing), Peking–Yale Joint Center for Plant Molecular Genetics and Agrobiotechnology, College of Life Sciences, Peking University, Beijing 100871, PR China

*Corresponding author: E-mail, liyi@pku.edu.cn; Fax, +86-10-62756903

(Received March 24, 2010; Accepted June 13, 2010)

The silent information regulator protein (Sir2) and its homologs are NAD⁺-dependent deacetylase enzymes that play important roles in a variety of physiological processes. However, the functions of the Sir2 family in plants are poorly understood. Here, we report that Arabidopsis AtSRT2, a homolog of yeast Sir2, negatively regulates plant basal defense against the pathogen *Pseudomonas syringae* pv. *tomato* DC3000 (*PstDC3000*). In response to *PstDC3000* infection, the expression of AtSRT2 was down-regulated in a salicylic acid (SA)-independent manner. In addition, knock-out of AtSRT2 (*srt2*) enhanced resistance against *PstDC3000* and increased expression of pathogenesis-related gene 1 (*PR1*). Conversely, overexpression of AtSRT2 resulted in hypersusceptibility to *PstDC3000* and impaired *PR1* induction. Consistent with this phenotype, expression of *PAD4*, *EDS5* and *SID2*, three essential genes in the SA biosynthesis pathway, were increased in the *srt2* mutant and decreased in AtSRT2-overexpressing plants. Taken together, these results demonstrate that AtSRT2 is a negative regulator of basal defense, possibly by suppressing SA biosynthesis.

Keywords: AtSRT2 • Basal defense • EDS5 • PAD4 • PstDC3000 • SID2.

Abbreviations: CaMV, cauliflower mosaic virus; DIG, digoxigenin; EDS1, enhanced disease susceptibility 1; EDS5, enhanced disease susceptibility 5; GFP, green fluorescent protein; HDAC, histone deacetylase; HR, hypersensitive response; GUS, β -glucuronidase; MS, Murashige and Skoog; NahG, salicylate hydroxylase; NPR1, non-expresser of PR genes 1; PAD4, phytoalexin deficient 4; PEG, polyethylene glycol; PR, pathogenesis-related; *PstDC3000*, *Pseudomonas syringae* pv. *tomato* DC3000; RT-PCR, reverse transcription-PCR; SA, salicylic acid; SID2, salicylic acid induction deficient 2; Sir2, silent information regulator 2; WT, wild type.

Nucleotide sequence data for the genes described in this study have been deposited in the GenBank/EMBL data libraries with

the following accession numbers: AtSRT2 (At5g09230); AtSRT1 (At5g55760); PAD4 (At3g52430); EDS5 (At4g39030); EDS1 (At3g48090); SID2 (At1g74710); NPR1 (At1g64280); PR1 (At2g14610).

Introduction

Silent information regulator 2 (Sir2) proteins, or sirtuins, are NAD⁺-dependent histone deacetylases (HDACs); NAD⁺ is required as a cofactor to deacetylate substrates (Blander and Guarente 2004, Dali-Youcef et al. 2007). Sir2 proteins contain sirtuin core domains, which are conserved from bacteria to humans (Brachmann et al. 1995, Frye 1999). Functional studies in yeast and mammalian cells have revealed that Sir2 proteins deacetylate both histone and non-histone substrates (Buck et al. 2004, Haigis and Guarente 2006, Sauve et al. 2006) and play important roles in numerous processes, including chromatin silencing, DNA repair, cell cycle, apoptosis and aging (Robyr et al. 2002, Blander and Guarente 2004, Yamamoto et al. 2007).

However, the functions of Sir2 proteins in plants are not fully understood. Sequence analysis has identified two Sir2 family genes in Arabidopsis (*AtSRT1* and *AtSRT2*) and rice (*OsSRT1* and *OsSRT2*) (Pandey et al. 2002). *AtSRT1* and *OsSRT1* belong to the same class of HDACs and showed a high sequence similarity (Pandey et al. 2002). Down-regulation of *OsSRT1* by RNA interference (RNAi) enhances histone H3K9 acetylation on transposable elements and promoters of hypersensitive response (HR)-related genes (Huang et al. 2007). This increased H3K9 acetylation triggers HR-related gene expression and leads to hydrogen peroxide production, DNA fragmentation, cell death and lesions mimicking plant HR (Huang et al. 2007). Studies of *OsSRT1* highlight the roles of plant Sir2 proteins in suppressing gene expression via histone H3 deacetylation. However, sequence analysis indicates that *AtSRT2* and *OsSRT1* are highly divergent, suggesting they may have different functions. The role of *AtSRT2* is not clear, although a recent study has shown that mutation of *AtSRT2* affects the Arabidopsis vernalization response (Bond et al. 2009).

Plant Cell Physiol. 51(8): 1291–1299 (2010) doi:10.1093/pcp/pcq087, available online at www.pcp.oxfordjournals.org

© The Author 2010. Published by Oxford University Press on behalf of Japanese Society of Plant Physiologists.

This is an Open Access article distributed under the terms of the Creative Commons Attribution Non-Commercial License (<http://creativecommons.org/licenses/by-nc/2.5>), which permits unrestricted non-commercial use distribution, and reproduction in any medium, provided the original work is properly cited.

Plants possess a complex network of defense strategies to deal with microbial pathogens. The small plant hormone molecule salicylic acid (SA) plays important roles in plant disease resistance. After detecting microbial pathogens, plants accumulate SA (Loake and Grant 2007, Vlot et al. 2008), which subsequently activates NPR1 (NON-EXRESSER OF PR GENES 1) and results in defensive reaction including the expression of pathogen-related (PR) genes (Cao et al. 1997). Biosynthesis of SA in response to pathogens is believed to be controlled by PAD4 (PHYTOALEXIN DEFICIENT 4), EDS5 (ENHANCED DISEASE SUSCEPTIBILITY 5) and SID2 (SALICYLIC ACID INDUCTION DEFICIENT 2) (Shah 2003). PAD4 encodes a lipase-like protein that interacts with EDS1 (ENHANCED DISEASE SUSCEPTIBILITY 1) (Jirage et al. 1999, Feys et al. 2001). EDS5 is homologous to the bacterial multidrug and toxin extrusion transporter (MATE) protein and may be involved in transporting SA precursors (Nawrath et al. 2002, Shah 2003). SID2 encodes isochorismate synthase (ICS1), which controls pathogen-induced SA biosynthesis (Wildermuth et al. 2001). SA levels are significantly lower in *pad4*, *eds5* and *sid2* mutants compared with wild-type (WT) plants (Zhou et al. 1998, Nawrath and Metraux 1999, Wildermuth et al. 2001). As a result, *pad4*, *eds5* and *sid2* mutants are hypersusceptible to biotrophic pathogens and are deficient in PR1 induction (Rogers and Ausubel 1997, Zhou et al. 1998, Nawrath and Metraux 1999).

Transcription defense genes are tightly regulated because numerous transcription factors interact to fine-tune the defense response (Riechmann et al. 2000, Thilmony et al. 2006). In addition, eukaryotic DNA is wrapped around histone octamers. The resulting chromatin provides a higher level of regulation; chromatin configuration can be altered to allow or prevent transcription initiation (Nelissen et al. 2007). In both *Arabidopsis* and tobacco, SA-induced PR1 expression is associated with increased histone acetylation at the PR1 promoter (Butterbrodt et al. 2006, Mosher et al. 2006), indicating that histone acetylation regulates gene expression in the SA signaling pathway. Previous studies have shown that PAD4, EDS5 and SID2 are rapidly induced by pathogens (Jirage et al. 1999,

Wildermuth et al. 2001, Nawrath et al. 2002). However, the mechanism by which transcription of PAD4, EDS5 and SID2 is regulated at the level of histone modification remains largely unclear.

In the present study, we characterized the functions of *Arabidopsis* deacetylase AtSRT2. We found that AtSRT2 was down-regulated by *Pseudomonas syringae* pv. *tomato* DC3000 (*Pst*DC3000) infection. The protein encoded by AtSRT2 negatively regulates the plant basal defense and PR1 expression. Moreover, pathogen-induced expression of PAD4, EDS5 and SID2 was suppressed by AtSRT2, suggesting that AtSRT2 plays an important role in regulating SA synthesis.

Results

Nuclear localization of AtSRT2

Several HDACs are translocated to the nucleus to regulate gene expression (Hollender and Liu 2008), which is consistent with their functions in modifying chromatin. AtSRT2 has seven predicted splice variants (see [Supplementary Fig. S1A](#)); however, only the third transcript (AtSRT2-CDS3), which lacks the two C-terminal exons, has been characterized (Pandey et al. 2002). We amplified the seven putative transcripts of AtSRT2 by reverse transcription-PCR (RT-PCR), and found that AtSRT2-CDS3 was the predominant splice variant (data not shown).

Sequence analysis has demonstrated that AtSRT2-CDS3 contains a typical nuclear localization signal (NLS) (Pandey et al. 2002). To determine the subcellular localization of AtSRT2-CDS3, we fused AtSRT2-CDS3 in-frame to the 5' end of the green fluorescent protein (dGFP). The AtSRT2-CDS3-dGFP construct was introduced into *Arabidopsis* mesophyll protoplasts by polyethylene glycol (PEG)-mediated DNA transfection (Yoo et al. 2007). Green fluorescence was detected in the whole cell transformed with the GFP control ([Fig. 1](#), upper panel), whereas the AtSRT2-CDS3-dGFP fusion protein was expressed exclusively in the nucleus ([Fig. 1](#), lower panel), indicating that AtSRT2-CDS3 localizes to the nucleus.

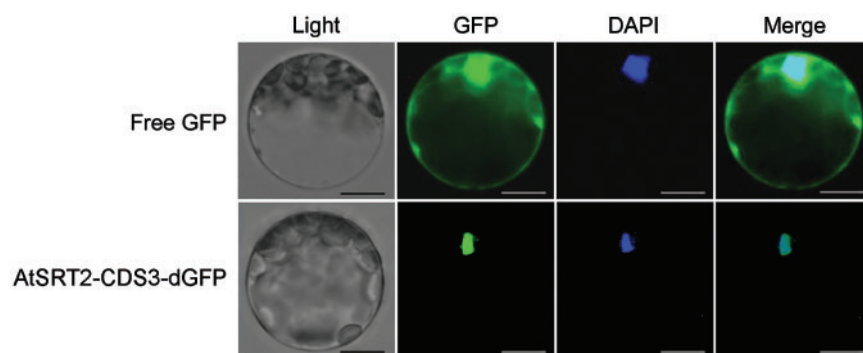


Fig. 1 Nuclear localization of AtSRT2-CDS3. Plasmids carrying green fluorescent protein (GFP control; upper panel) or AtSRT2-CDS3-GFP (bottom panel) were transformed into *Arabidopsis* mesophyll protoplasts. Fluorescent images were taken at 16 h after transfection. The nucleus was stained with 4',6-diamidino-2-phenylindole (DAPI). Scale bar = 10 μ m. The image is representative of experiments performed in triplicate.

Expression profile of AtSRT2

To determine the function of AtSRT2, we first evaluated its expression profile by fusing the AtSRT2 promoter to a β -glucuronidase (GUS) reporter gene. The resulting construct (pAtSRT2-GUS) was transformed into Arabidopsis. Four independent transgenic lines with a single insertion were obtained, and GUS activity was detected in different organs and development stages (Fig. 2A–F). In particular, AtSRT2 promoter activity was high in roots (Fig. 2A, 2B), leaves (Fig. 2B, D) and flowers (Fig. 2E).

To assess whether the expression of AtSRT2 is responsive to pathogen infection, we compared GUS activity in transgenic plants before and after virulent *PstDC3000* inoculation. GUS activity was reduced after pathogen inoculation but not after mock treatment (Fig. 2G, H), which suggests that *PstDC3000* infection represses AtSRT2 expression.

Down-regulation of AtSRT2 by *PstDC3000*, inoculation

The down-regulation of AtSRT2 promoter activity by *PstDC3000* infection (Fig. 2G, H) prompted us to evaluate the role of AtSRT2 in the plant basal defense. To gain more detailed insights into AtSRT2 expression upon *PstDC3000* infection, we determined AtSRT2 mRNA levels by quantitative RT-PCR in *PstDC3000*-inoculated plants at different time points. As shown in Fig. 3A, pathogen infection markedly reduced AtSRT2 mRNA levels. Only about 30% of AtSRT2 transcripts remained at 24 h after pathogen inoculation, which is consistent with our promoter activity assay results (Fig. 2).

The SA-mediated signaling pathway regulated by NPR1 is one of the most important pathways in plant defense (Durrant and Dong 2004, Loake and Grant 2007). To assess the roles of SA and NPR1 in the pathogen-induced down-regulation of AtSRT2, we determined AtSRT2 mRNA levels in the *npr1-3* mutant and SA-deficient *NahG* transgenic plants. As shown in Fig. 3B, AtSRT2 expression was still inhibited by *PstDC3000* infection in *npr1-3* mutants and *NahG* plants, indicating that AtSRT2 expression is not dependent on SA or NPR1. Consistent with this result, we also found that the AtSRT2 mRNA levels were not affected by exogenous SA treatment in WT plants (Fig. 3C).

Disruption of AtSRT2 enhances plant basal defense and PR1 expression

To characterize the functions of AtSRT2 in vivo, we obtained a homozygous T-DNA insertion line (SALK_149295) for AtSRT2 from the Arabidopsis Biological Resource Center (ABRC). The precise insertion position was determined by PCR with primers specific to AtSRT2 and the T-DNA sequence, followed by sequencing of the PCR product. We found that SALK_149295 carries a T-DNA insertion in the second exon of AtSRT2 (see Supplementary Fig. S1A). AtSRT2 mRNA was not detected in the *srt2* mutant by RT-PCR (see Supplementary Fig. S1B).

The down-regulation of AtSRT2 by pathogen infection prompted us to investigate the potential role of AtSRT2 in regulating the plant basal defense. After inoculating the *srt2* mutant and WT plants with *PstDC3000*, we compared bacterial growth rates. As shown in Fig. 4A, at 0 day post-inoculation (dpi),

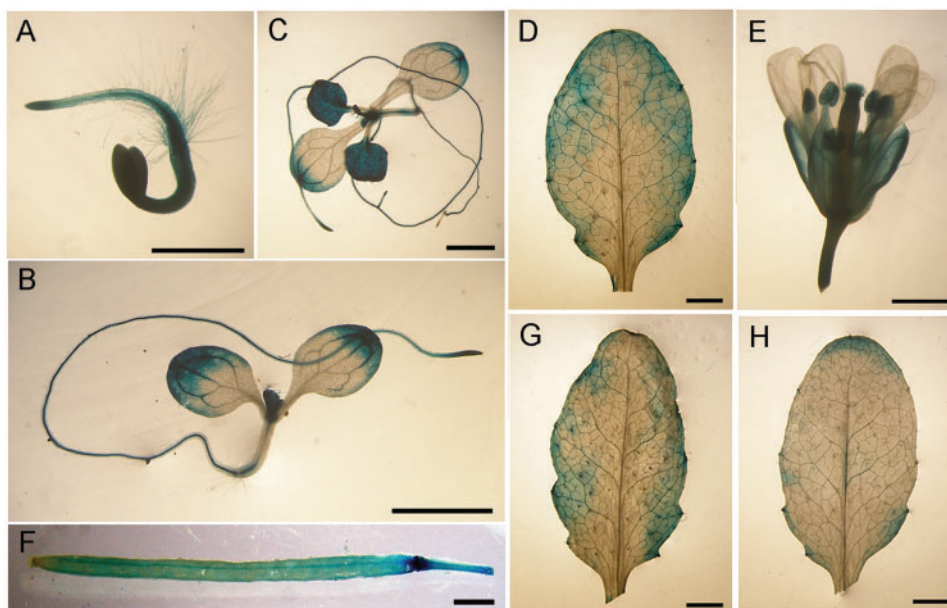


Fig. 2 Expression profile of AtSRT2. β -Glucuronidase (GUS) activity was detected by histochemistry in transgenic plants containing pAtSRT2-GUS. Typical GUS expression patterns are shown for (A) 3-day-old seedlings; (B) 6-day-old seedlings; (C) 12-day-old seedlings; (D) leaves from adult plants; (E) flowers; (F) siliques; (G) mock-treated leaves; and (H) leaves inoculated with *PstDC3000*. Scale bar = 1 mm. These images are representative of experiments performed in triplicate.

srt2 and WT plants contained the same amount of *Pst*DC3000, indicating equal initial bacterial doses. However, at 3 dpi, the bacterial pathogen accumulated in the *srt2* mutant was 10-fold lower than that of WT plants in three independent experiments, suggesting that the *srt2* mutation enhanced the plant

basal defense. *PR* genes have been widely used as markers of the plant basal defense system (Durrant and Dong 2004). We determined *PR1* mRNA expression in *Pst*DC3000-inoculated *srt2* and WT plants by quantitative RT-PCR and Northern blot. As shown in Fig. 4B and Supplementary Fig. S2, *Pst*DC3000

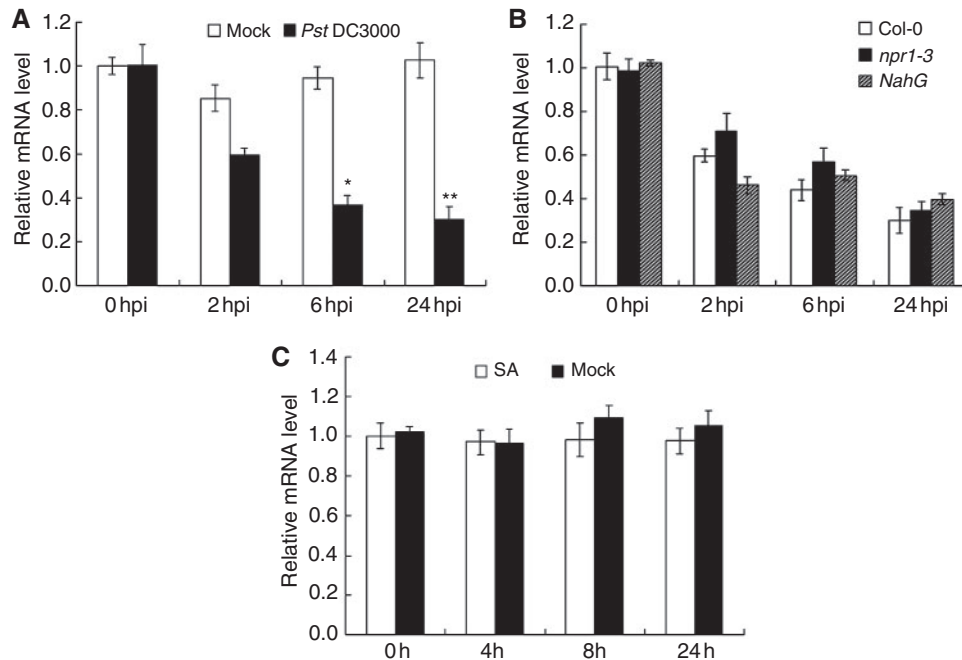


Fig. 3 *AtSRT2* expression is repressed by pathogen infection. (A) Four-week-old WT Arabidopsis plants (Col-0) were infiltrated with 10 mM $MgCl_2$ (open bars) or *Pst*DC3000 (filled bars; $OD_{600} = 0.2$ in 10 mM $MgCl_2$). The infiltrated leaves were collected at the indicated time for quantitative RT-PCR analysis. (B) Four-week-old WT (Col-0), *npr1-3* and *NahG* Arabidopsis plants were infiltrated with *Pst*DC3000 ($OD_{600} = 0.2$ in 10 mM $MgCl_2$). The infiltrated leaves were collected at the indicated time for quantitative RT-PCR analysis. (C) Two-week-old WT (Col-0) seedlings grown on MS medium were untreated (open bars) or treated with 0.5 mM salicylic acid (SA; filled bars). Seedlings were collected at the indicated time for quantitative RT-PCR analysis. *UBQ10* was used as an internal control. Data represent the mean \pm SD from four independent experiments. The statistical significance of the difference was confirmed by Student's *t*-test, * $P < 0.05$; ** $P < 0.01$.

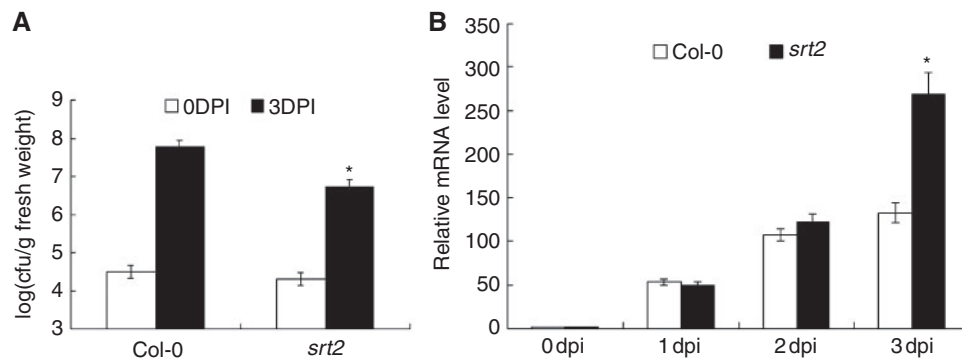


Fig. 4 The *srt2* mutant is more resistant to pathogen infection. (A) WT (Col-0) plants and *srt2* mutants were infiltrated with a suspension of *Pst*DC3000 ($OD_{600} = 0.0001$ in 10 mM $MgCl_2$). Bacterial growth was determined at 0 dpi (open bars) or 3 dpi (filled bars). Each data point consisted of at least six samples. Error bars indicate the SD. The statistical significance of the difference was confirmed by Student's *t*-test, * $P < 0.05$. (B) Pathogen-induced *PR1* expression. WT (Col-0) plants and *srt2* mutants were infiltrated with a suspension of *Pst*DC3000 ($OD_{600} = 0.0001$ in 10 mM $MgCl_2$). Total RNA was extracted at the time indicated for quantitative RT-PCR analysis. *UBQ10* was used as internal control. Data represent the mean \pm SD from three independent experiments. The statistical significance of the difference was confirmed by Student's *t*-test, * $P < 0.05$.

treatment induced *PR1* expression strongly in both WT and mutant plants, and *PR1* transcripts levels were higher in *srt2* mutants at 3 dpi compared with the WT.

Overexpression of *AtSRT2-CDS3* compromises plant basal defense and *PR1* expression

To characterize further the function of *AtSRT2* in the basal defense system, we generated transgenic *Arabidopsis* plants that overexpress *AtSRT2-CDS3*. The *AtSRT2-CDS3* full-length cDNA was cloned behind the cauliflower mosaic virus (CaMV) 35S promoter, and this construct was transformed into *Arabidopsis* plants. Three independent transgenic lines (OE2, OE7 and OE15) were chosen for further analysis. Our quantitative RT-PCR results revealed constitutively elevated expression of *AtSRT2* in all the three transgenic plants, while the expression level of *AtSRT2* in OE2 was lower than that in OE7 and OE15 (Fig. 5A).

After *PstDC3000* inoculation of plants, more bacterial pathogen was detected in the overexpressing transgenic lines compared with WT plants at 3 dpi in three independent experiments (Fig. 5B), indicating that overexpression of *AtSRT2-CDS3* made plants more susceptible to *PstDC3000* infection. In addition, OE2 was susceptible to *PstDC3000* at a similar level to that of OE7 and OE15, suggesting that pathogen susceptibility in overexpressing plants might be independent of the expression level of *AtSRT2*. Consistent with these findings, *PR1* transcripts were reduced in the *AtSRT2*-overexpressing lines compared with WT plants (Fig. 5C and Supplementary Fig. S2). These results are consistent with our findings in the *srt2* mutant. Thus, analysis of both loss-of-function *AtSRT2* mutants and gain-of-function *AtSRT2-CDS3*-overexpressing plants indicates that *AtSRT2* functions as a negative regulator in plant basal defense.

Besides pathogen inoculation, we also analyzed SA-induced *PR1* expression in WT, *srt2* and *AtSRT2-CDS3*-overexpressing

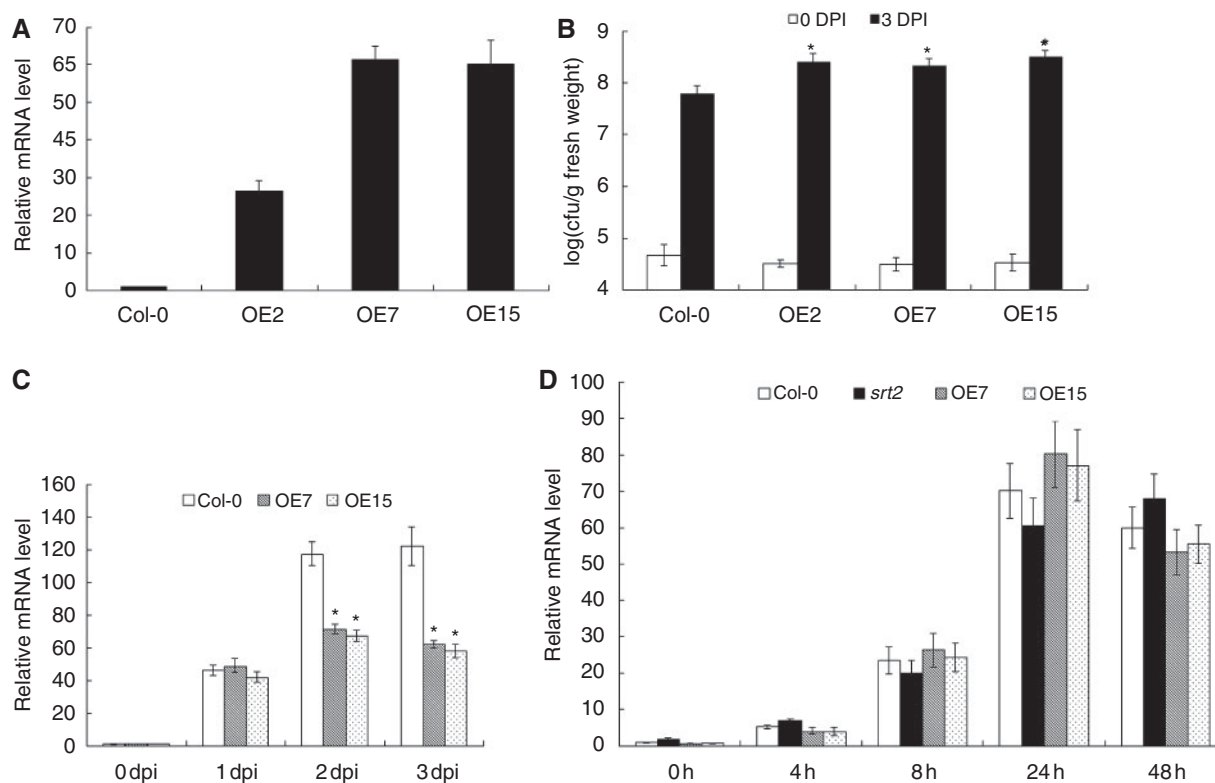


Fig. 5 Overexpression of *AtSRT2-CDS3* attenuates the plant defense response. (A) *AtSRT2* expression of 4-week-old WT (Col-0) and *AtSRT2-CDS3*-overexpressing *Arabidopsis* plants was determined by quantitative RT-PCR. *UBQ10* was used as an internal control. Data represent the mean \pm SD from two independent experiments. (B) WT (Col-0) and *AtSRT2-CDS3*-overexpressing plants were infiltrated with a suspension of *PstDC3000* ($OD_{600} = 0.0001$ in 10 mM $MgCl_2$). Samples were taken at 0 dpi (open bars) or 3 dpi (filled bars) to determine bacterial growth. Each data point consisted of at least six samples. Error bars indicate the SD. The statistical significance of the difference was confirmed by Student's *t*-test, * $P < 0.05$. (C) Pathogen-induced *PR1* expression. WT (Col-0) and *AtSRT2-CDS3*-overexpressing plants (OE7 and OE15) were treated with a suspension of *PstDC3000* ($OD_{600} = 0.0001$ in 10 mM $MgCl_2$). Inoculated leaves were collected for quantitative RT-PCR analysis. *UBQ10* was used as internal control. Data represent the mean \pm SD from three independent experiments. The statistical significance of the difference was confirmed by Student's *t*-test, * $P < 0.05$. (D) Two-week-old WT (Col-0), *srt2* and *AtSRT2-CDS3*-overexpressing (OE7 and OE15) *Arabidopsis* plants were treated with 0.5 mM SA to induce *PR1* expression. Total RNA was extracted at different time points for quantitative RT-PCR analysis. *UBQ10* was used as internal control. Data represent the mean \pm SD from two independent experiments.

plants to determine the mechanism by which AtSRT2 regulates the SA signaling pathway. As shown in Fig. 5D, we did not see a significant difference in *PR1* transcript levels among WT, *srt2* mutant and overexpression plants, suggesting that AtSRT2 does not influence downstream gene expression in the presence of SA.

AtSRT2 negatively regulates *EDS5*, *PAD4* and *SID2* expression

Biosynthesis of SA, which requires a series of enzymes, is an essential step in the plant defense against biotrophic pathogens (Shah 2003, Durrant and Dong 2004). We found that AtSRT2 repressed pathogen-induced *PR1* expression but had little effect on SA-induced *PR1* expression (Figs. 4B, 5C, D), suggesting that AtSRT2 is involved downstream of pathogen recognition but upstream of SA signaling. To better understand the role of AtSRT2 in SA biosynthesis in the plant basal defense system, we analyzed the expression of SA biosynthesis-related enzymes *PAD4*, *EDS5* and *SID2* under various conditions. As shown in Fig. 6, expression of *PAD4*, *EDS5* and *SID2* at 0 dpi was higher in the *srt2* mutant but lower in AtSRT2-CDS3-overexpressing lines compared with the WT, suggesting that these three genes are repressed by AtSRT2 even in the absence of pathogens. Treatment with *PstDC3000* increased expression of *PAD4*, *EDS5* and *SID2*, which is consistent with results of previous studies (Jirage et al. 1999, Wildermuth et al. 2001, Nawrath et al. 2002). Furthermore, pathogen-induced expression of all the three genes was significantly higher in *srt2* plants but lower in

AtSRT2-CDS3-overexpressing plants compared with the WT (Fig. 6). Taken together, these results indicate that AtSRT2 negatively regulates both basal and pathogen-induced expression of SA biosynthesis-related genes, possibly a determinant for its role in suppressing plant basal defense.

Discussion

Histone modification, especially acetylation, is essential for transcriptional regulation. In general, histone hyperacetylation is associated with gene activation, whereas histone deacetylation by HDACs leads to gene repression (Hebbes et al. 1988, Hollender and Liu 2008). Plant genomes contain a large number of HDACs (Pandey et al. 2002), making it important, but challenging, to determine the function of each specific HDAC.

Our findings also demonstrated that AtSRT2 functions as a negative regulator of the plant basal defense. First, we generated transgenic Arabidopsis plants that stably expressed the *GUS* gene under the control of the AtSRT2 promoter. *GUS* staining was observed in roots (Fig. 2A, B), leaves (Fig. 2B, D) and flowers (Fig. 2E). AtSRT2 was found to affect the expression of *FLC* and the vernalization response of Arabidopsis (Bond et al. 2009). Our *GUS* staining result suggested that AtSRT2 may have effects on plant growth and development. *GUS* staining also revealed that AtSRT2 promoter activity was reduced upon *PstDC3000* inoculation (Fig. 2G, H), indicating that AtSRT2 may be involved in the *PstDC3000*-induced defense

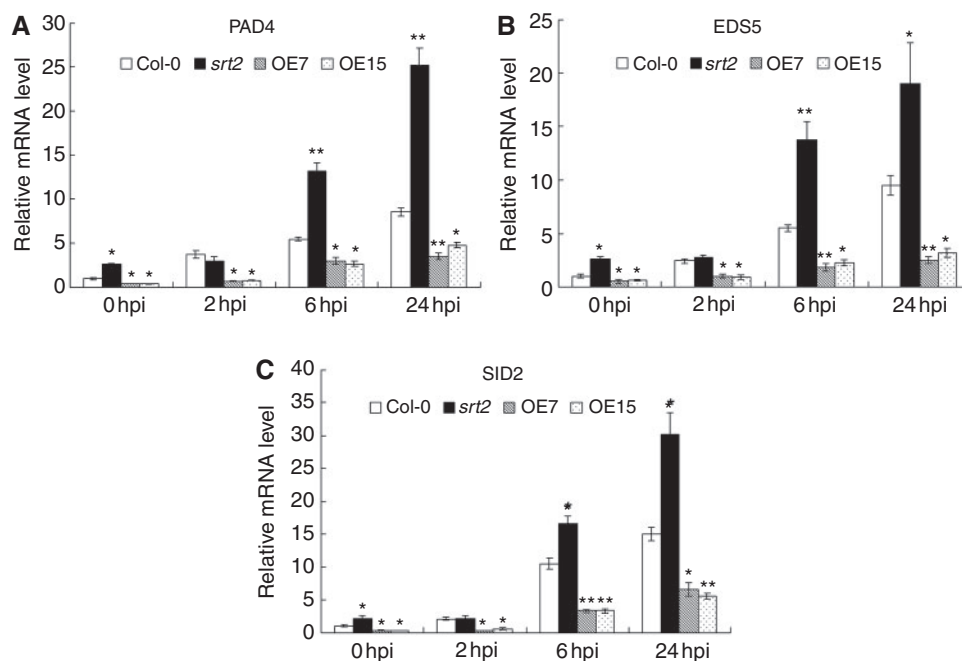


Fig. 6 AtSRT2 negatively regulates *EDS5*, *PAD4* and *SID2* expression. Four-week-old WT (Col-0), *srt2* and AtSRT2-CDS3-overexpressing (OE7 and OE15) Arabidopsis plants were inoculated with *PstDC3000* ($OD_{600} = 0.2$ in 10 mM $MgCl_2$). Total RNA was extracted at the indicated time points for quantitative RT-PCR analysis of *PAD4*, *EDS5* and *SID2*. *UBQ10* was used as an internal control. Data represent the mean \pm SD from three independent experiments. The statistical significance of the difference was confirmed by Student's *t*-test, * $P < 0.05$, ** $P < 0.01$.

response. Quantitative RT-PCR analysis confirmed that *AtSRT2* expression was repressed by *PstDC3000* infection (Fig. 3A, B) in an NPR1- and SA-independent manner (Fig. 3B, C).

Secondly, knock-out of *AtSRT2* enhanced resistance against *PstDC3000* infection and increased *PR1* expression (Fig. 4 and Supplementary Fig. S2), suggesting a negative regulatory role for *AtSRT2* in the pathogen-induced defense response. This conclusion was supported by findings in *AtSRT2-CDS3*-overexpressing plants; both independent homozygous transgenic lines were more susceptible to *PstDC3000* infection (Fig. 5B) and attenuated *PstDC3000*-induced *PR1* expression (Fig. 5C and Supplementary Fig. S2).

Thirdly, pathogen-induced expression of *PAD4*, *EDS5* and *SID2*, three key regulators of SA biosynthesis, was increased in the *srt2* mutant but markedly reduced in *AtSRT2-CDS3*-overexpressing lines compared with WT plants (Fig. 6). The *AtSRT2* attenuation of SA biosynthesis-related genes indicates suppression of SA-mediated signaling. Further, exogenous SA treatment did not affect *AtSRT2* expression (Fig. 3C), and exogenous SA-induced *PR1* expression was unaffected by the *srt2* mutation or overexpression (Fig. 5D). We also studied the potential function of *AtSRT2* in response to an avirulent strain of *PstDC3000*. We measured the ionic conductivity of the released electrolyte after *PstDC3000* (AvrRpt2) infection but did not observe any significant difference among WT, *srt2* and *AtSRT2-CDS3*-overexpressing plants (data not shown).

In the present study, we characterized the function of *AtSRT2*, which is a member of the second HDAC subfamily in *Arabidopsis*. *AtSRT2* has seven predicted splice variants (Pandey et al. 2002); we observed that the third transcript (*AtSRT2-CDS3*) was the predominant splice variant (data not shown). In addition, we showed that the *AtSRT2-CDS3*-dGFP fusion protein was located exclusively in the nucleus (Fig. 1), suggesting a role for *AtSRT2-CDS3* in regulating gene expression.

SA is essential in plant disease resistance. In response to hemi-biotrophic pathogens such as *PstD3000*, plants accumulate SA and rapidly activate SA signaling (Nimchuk et al. 2003, Akira et al. 2006). However, SA itself can be harmful to the growth, reproduction and survival of plants, especially at high doses (Heil and Baldwin 2002). In *Arabidopsis*, constitutive overproduction of SA results in a strongly dwarfed phenotype and decreased seed production (Mauch et al. 2001). Thus negative regulation of SA biosynthesis-related genes is needed to avoid SA toxicity (Heil and Baldwin 2002). Expression of *PAD4*, *EDS5* and *SID2* was enhanced in the *srt2* mutant but reduced in the *AtSRT2-CDS3*-overexpressing lines; therefore, we propose that *AtSRT2* inhibits SA accumulation by suppressing SA biosynthesis-related genes. The antagonistic effects of *AtSRT2* on SA synthesis may prevent an effective response to pathogen infections (Figs. 4A, 5B); therefore, negative regulation of *AtSRT2* expression occurs as early as 2 h after pathogen inoculation (Fig. 3A). However, the mechanism by which *AtSRT2* is regulated at this early stage of the defense response requires further investigation.

Numerous HDACs suppress gene expression by reducing histone acetylation (Hollender and Liu 2008). OsSRT1, an SIR2-related protein in rice, was found to deacetylate histone H3K9 and repress HR-related genes (Huang et al. 2007). Our results indicate that *AtSRT2* negatively regulates the plant basal defense, presumably by down-regulating *PAD4*, *EDS5* and *SID2* expression. Sequence similarity among *AtSRT2* and other SIR2 family members suggests that *AtSRT2* may negatively regulate *PAD4*, *EDS5* and *SID2* by histone deacetylation of their promoters.

The understanding of plant defense regulation is still limited. In particular, the balance between activation and deactivation of defense-related genes to fine-tune the plant basal defense response remains largely unclear. Our results demonstrate that *AtSRT2* attenuates the plant basal defense by reducing SA biosynthesis-related gene expression, providing insights into deactivation of SA signaling in the plant basal defense.

Materials and Methods

Plant materials

Seeds of *Arabidopsis thaliana* ecotype Columbia (Col-0) were surface-sterilized with 10% NaClO for 15 min and then washed five times with sterile water. Sterile seeds were suspended in 0.12% agarose and plated on Murashige and Skoog (MS) medium (Murashige and Skoog 1962) plus 3% sucrose. Plants were stratified in the dark for 48 h at 4°C and then grown in a controlled growth chamber with a relatively short photoperiod (10 h light at 22°C/14 h dark at 20°C) with approximately 75% relative humidity. After 2 weeks, seedlings were potted in soil.

Isolation of the T-DNA insertion mutant

Seeds of WT *Arabidopsis* and the *srt2* mutant (SALK_149295) were obtained from the ABRC. The homozygous mutant was isolated according to the Salk protocol (<http://signalsalk.edu/tdnaprimers.2.html>). Plants homozygous for the T-DNA insertion were confirmed by PCR amplification using primers corresponding to the sequences flanking the T-DNA insertion and gene-specific primers. Primer sequences are shown in Supplementary Table S1.

Overexpression

The sequence of *AtSRT2-CDS3* was amplified from the cDNA of WT (Col-0) plants using a high-fidelity DNA polymerase, KOD-plus (Toyobo, Osaka, Japan). Forward and reverse primer sequences are shown in Supplementary Table S1. The PCR product was inserted into the *NcoI* restriction sites of vector pRTL2-dGFP (a derivative of pRTL2). The coding sequence of *AtSRT2* was fused in-frame to the N-terminus of the first GFP-coding sequence and driven by the CaMV 35S promoter. The resulting *pRTL2-AtSRT2-dGFP* construct was also used in the cellular localization assay. A restriction fragment containing *AtSRT2* was released from *pRTL2-AtSRT2-dGFP* using *HindIII* and ligated into the binary vector

pCAMBIA 1301 (<http://www.cambia.org>). The binary plasmid pCAMBIA1301-AtSRT2 was transformed into *Agrobacterium tumefaciens* strain GV3101 (pMP90).

Arabidopsis transformation was performed with the floral dip method (Clough and Bent 1998). To screen for transformants, seeds were grown on MS medium plates containing 40 $\mu\text{g ml}^{-1}$ hygromycin B (Roche Diagnostics, Mannheim, Germany). Resistant plants were transferred to soil for further analysis.

Chemical treatment

Two-week-old seedlings grown on MS medium were transferred to fresh MS solution containing 0.5 mM SA (Sigma, USA). Samples were collected at different time points.

Northern blot

Total RNA was isolated from treated plants with TRIzol reagent (Invitrogen, USA) according to the manufacturer's instructions. Approximately 5 μg of total RNA from each sample was separated on a 1.2% formaldehyde agarose gel (Mao et al. 2007). After transferring the separated RNA to Hybond-N membranes (Amersham Biosciences, UK), the membranes were hybridized with digoxigenin (DIG)-labeled probes. Immunodetection was performed according to the manufacturer's instructions (Roche).

Pathogen inoculation

Pseudomonas syringae pv. *tomato* DC3000 strain was propagated at 28°C on King's B medium containing rifampicin (50 $\mu\text{g ml}^{-1}$). For disease testing, at least six 4-week-old plants were infiltrated with 10 mM MgCl_2 (mock treatment) or a bacterial suspension of PstDC3000 ($\text{OD}_{600} = 0.0001$ in 10 mM MgCl_2). After 3 d, leaves were harvested, homogenized in 10 mM MgCl_2 and then serially diluted and spread on King's B medium containing rifampicin (50 $\mu\text{g ml}^{-1}$). Plates were incubated at 28°C for 2 d, and the colony number was then determined. Data analyses were performed using the computer program Sigma Plot Version 10.0 software and were considered significantly different at the 0.05 level. To determine expression of AtSRT2, PAD4, EDS5 and SID2, a bacterial suspension of PstDC3000 ($\text{OD}_{600} = 0.2$ in 10 mM MgCl_2) was used.

Quantitative RT-PCR

Total RNA was extracted with Trizol Reagent (Invitrogen) and treated with RNase-free DNase I (TAKARA Biotechnology, Dalian, China). First-strand cDNA was synthesized with SuperScript III Reverse Transcriptase (Invitrogen) and then diluted for use as template for quantitative RT-PCR. Primer sequences are shown in [Supplementary Table S1](#). PCR was carried out using SYBR Green Real-time PCR Master Mix (Toyobo, Japan) on an Opticon 2 continuous fluorescence detection system (CFD-3220, MJ Research, USA). The specific mRNA abundance relative to constitutively expressed UBQ10 was calculated using the $2^{-\Delta\Delta\text{Ct}}$ method (Livak and Schmittgen 2001, Ferreira et al. 2006).

Histochemical GUS detection

To generate the pAtSRT2-GUS construct, a 1.2 kb fragment upstream of the AtSRT2 gene was amplified by PCR from genomic DNA. After sequence analysis, the promoter fragment was cloned into pCAMBIA1300-221 (Chu et al. 2007). Four independent transgenic lines, each containing a single T-DNA insertion, were tested for GUS activity. Tissues were incubated overnight in GUS staining buffer [2 mM X-gluc, 0.1 M sodium phosphate buffer (pH 7.0), 0.1% Triton X-100, 1 mM potassium ferricyanide, 1 mM potassium ferrocyanide, 10 mM EDTA] at 37°C in the dark. Samples were destained with 75% ethanol solution and examined by a light microscope (Olympus SZX-ILLD2-200, Olympus Corporation, Tokyo, Japan).

Cellular localization assay

The pRTL2-AtSRT2-dGFP plasmid was introduced into Arabidopsis mesophyll protoplasts; pRTL2-dGFP was used as a control with the DNA-PEG-calcium method as described previously (Yoo et al. 2007). After transfection, protoplasts were maintained for 16 h at room temperature in the dark. GFP was detected by fluorescence microscopy (Type 020-525.021, Leica Microsystems Ltd., Germany) and photographed with a KX Series Imaging System (Model KX32E, Apogee Instruments Inc., Logan, UT, USA).

Supplementary data

Supplementary data are available at PCP online.

Funding

This work was supported by grants from 973 [contract No. 2006CB101905, 2007CB10920204 programs to Y.L.]

Acknowledgments

We thank the ABRC for *srt2* seeds, Dr. Biao Ding for pRTL2:dGFP (dimeric GFP), and Dr. Qi Xie for pCambia 1300-221. The virulent pathogen PstDC3000 was kindly provided by Dr. Jian-Min Zhou.

References

- Akira, S., Uematsu, S. and Takeuchi, O. (2006) Pathogen recognition and innate immunity. *Cell* 124: 783–801.
- Blander, G. and Guarente, L. (2004) The Sir2 family of protein deacetylases. *Annu. Rev. Biochem.* 73: 417–435.
- Bond, D.M., Dennis, E.S., Pogson, B.J. and Finnegan, E.J. (2009) Histone acetylation, VERNALIZATION INSENSITIVE 3, FLOWERING LOCUS C, and the vernalization response. *Mol. Plant* 2: 724–737.
- Brachmann, C.B., Sherman, J.M., Devine, S.E., Cameron, E.E., Pillus, L. and Boeke, J.D. (1995) The Sir2 gene family, conserved from bacteria to humans, functions in silencing, cell-cycle progression, and chromosome stability. *Genes Dev.* 9: 2888–2902.
- Buck, S.W., Gallo, C.M. and Smith, J.S. (2004) Diversity in the Sir2 family of protein deacetylases. *J. Leukoc. Biol.* 75: 939–950.
- Butterbrodt, T., Thurow, C. and Gatz, C. (2006) Chromatin immunoprecipitation analysis of the tobacco PR-1a- and the

- truncated CaMV 35S promoter reveals differences in salicylic acid-dependent TGA factor binding and histone acetylation. *Plant Mol. Biol.* 61: 665–674.
- Cao, H., Glazebrook, J., Clarke, J.D., Volko, S. and Dong, X.N. (1997) The Arabidopsis NPR1 gene that controls systemic acquired resistance encodes a novel protein containing ankyrin repeats. *Cell* 88: 57–63.
- Chu, Z., Chen, H., Zhang, Y., Zhang, Z., Zheng, N., Yin, B., et al. (2007) Knockout of the AtCESA2 gene affects microtubule orientation and causes abnormal cell expansion in Arabidopsis. *Plant Physiol.* 143: 213–224.
- Clough, S.J. and Bent, A.F. (1998) Floral dip: a simplified method for Agrobacterium-mediated transformation of Arabidopsis thaliana. *Plant J.* 16: 735–743.
- Dali-Youcef, N., Lagouge, M., Froelich, S., Koehl, C., Schoonjans, K. and Auwerx, J. (2007) Sirtuins: the 'magnificent seven', function, metabolism and longevity. *Ann. Med.* 39: 335–345.
- Durrant, W.E. and Dong, X. (2004) Systemic acquired resistance. *Annu. Rev. Phytopathol.* 42: 185–209.
- Ferreira, I.D., Rosario, V.E. and Cravo, P.V. (2006) Real-time quantitative PCR with SYBR Green I detection for estimating copy numbers of nine drug resistance candidate genes in Plasmodium falciparum. *Malaria J.* 5: 6.
- Feys, B.J., Moisan, L.J., Newman, M.A. and Parker, J.E. (2001) Direct interaction between the Arabidopsis disease resistance signaling proteins, EDS1 and PAD4. *EMBO J.* 20: 5400–5411.
- Frye, R.A. (1999) Characterization of five human cDNAs with homology to the yeast SIR2 gene: Sir2-like proteins (sirtuins) metabolize NAD and may have protein ADP-ribosyltransferase activity. *Biochem. Biophys. Res. Commun.* 260: 273–279.
- Haigis, M.C. and Guarente, L.P. (2006) Mammalian sirtuins—emerging roles in physiology, aging, and calorie restriction. *Genes Dev.* 20: 2913–2921.
- Hebbes, T.R., Thorne, A.W. and Cranerobinson, C. (1988) A direct link between core histone acetylation and transcriptionally active chromatin. *EMBO J.* 7: 1395–1402.
- Heil, M. and Baldwin, I.T. (2002) Fitness costs of induced resistance: emerging experimental support for a slippery concept. *Trends Plant Sci.* 7: 61–67.
- Hollender, C. and Liu, Z. (2008) Histone deacetylase genes in Arabidopsis development. *J Integr. Plant Biol.* 50: 875–885.
- Huang, L., Sun, Q., Qin, F., Li, C., Zhao, Y. and Zhou, D.X. (2007) Down-regulation of a SILENT INFORMATION REGULATOR2-related histone deacetylase gene, OsSRT1, induces DNA fragmentation and cell death in rice. *Plant Physiol.* 144: 1508–1519.
- Jirage, D., Tootle, T.L., Reuber, T.L., Frost, L.N., Feys, B.J., Parker, J.E., et al. (1999) Arabidopsis thaliana PAD4 encodes a lipase-like gene that is important for salicylic acid signaling. *Proc. Natl Acad. Sci. USA* 96: 13583–13588.
- Livak, K.J. and Schmittgen, T.D. (2001) Analysis of relative gene expression data using real-time quantitative PCR and the 2^{−(Delta Delta C(T))} method. *Methods* 25: 402–408.
- Loake, G. and Grant, M. (2007) Salicylic acid in plant defence—the players and protagonists. *Curr. Opin. Plant Biol.* 10: 466–472.
- Mao, P., Duan, M., Wei, C. and Li, Y. (2007) WRKY62 transcription factor acts downstream of cytosolic NPR1 and negatively regulates jasmonate-responsive gene expression. *Plant Cell Physiol.* 48: 833–842.
- Mauch, F., Mauch-Mani, B., Gaille, C., Kull, B., Haas, D. and Reimann, C. (2001) Manipulation of salicylate content in Arabidopsis thaliana by the expression of an engineered bacterial salicylate synthase. *Plant J.* 25: 67–77.
- Mosher, R.A., Durrant, W.E., Wang, D., Song, J.Q. and Dong, X.N. (2006) A comprehensive structure–function analysis of Arabidopsis SN1 defines essential regions and transcriptional repressor activity. *Plant Cell* 18: 1750–1765.
- Murashige, T. and Skoog, F. (1962) A revised medium for rapid growth and bioassays with tobacco tissue cultures. *Physiol. Plant.* 15: 473–477.
- Nawrath, C., Heck, S., Parinshawong, N. and Metraux, J.P. (2002) EDS5, an essential component of salicylic acid-dependent signaling for disease resistance in Arabidopsis, is a member of the MATE transporter family. *Plant Cell* 14: 275–286.
- Nawrath, C. and Metraux, J.P. (1999) Salicylic acid induction-deficient mutants of Arabidopsis express PR-2 and PR-5 and accumulate high levels of camalexin after pathogen inoculation. *Plant Cell* 11: 1393–1404.
- Nelissen, H., Boccardi, T.M., Himanen, K. and Van Lijsebettens, M. (2007) Impact of core histone modifications on transcriptional regulation and plant growth. *Crit. Rev. Plant Sci.* 26: 243–263.
- Nimchuk, Z., Eulgem, T., Holt, B.E. and Dangl, J.L. (2003) Recognition and response in the plant immune system. *Annu. Rev. Genet.* 37: 579–609.
- Pandey, R., Muller, A., Napoli, C.A., Selinger, D.A., Pikaard, C.S., Richards, E.J., et al. (2002) Analysis of histone acetyltransferase and histone deacetylase families of Arabidopsis thaliana suggests functional diversification of chromatin modification among multicellular eukaryotes. *Nucleic Acids Res.* 30: 5036–5055.
- Riechmann, J.L., Heard, J., Martin, G., Reuber, L., Jiang, C.Z., Keddie, J., et al. (2000) Arabidopsis transcription factors: genome-wide comparative analysis among eukaryotes. *Science* 290: 2105–2110.
- Robyr, D., Suka, Y., Xenarios, I., Kurdistani, S.K., Wang, A., Suka, N., et al. (2002) Microarray deacetylation maps determine genome-wide functions for yeast histone deacetylases. *Cell* 109: 437–446.
- Rogers, E.E. and Ausubel, F.M. (1997) Arabidopsis enhanced disease susceptibility mutants exhibit enhanced susceptibility to several bacterial pathogens and alterations in PR-1 gene expression. *Plant Cell* 9: 305–316.
- Sauve, A.A., Wolberger, C., Schramm, V.L. and Boeke, J.D. (2006) The biochemistry of sirtuins. *Annu. Rev. Biochem.* 75: 435–465.
- Shah, J. (2003) The salicylic acid loop in plant defense. *Curr. Opin. Plant Biol.* 6: 365–371.
- Thilmony, R., Underwood, W. and He, S.Y. (2006) Genome-wide transcriptional analysis of the Arabidopsis thaliana interaction with the plant pathogen Pseudomonas syringae pv. tomato DC3000 and the human pathogen Escherichia coli O157:H7. *Plant J.* 46: 34–53.
- Vlot, A.C., Klessig, D.F. and Park, S.W. (2008) Systemic acquired resistance: the elusive signal(s). *Curr. Opin. Plant Biol.* 11: 436–442.
- Wildermuth, M.C., Dewdney, J., Wu, G. and Ausubel, F.M. (2001) Isochorismate synthase is required to synthesize salicylic acid for plant defence. *Nature* 414: 562–565.
- Yamamoto, H., Schoonjans, K. and Auwerx, J. (2007) Sirtuin functions in health and disease. *Mol. Endocrinol.* 21: 1745–1755.
- Yoo, S.D., Cho, Y.H. and Sheen, J. (2007) Arabidopsis mesophyll protoplasts: a versatile cell system for transient gene expression analysis. *Nat. Protoc.* 2: 1565–1572.
- Zhou, N., Tootle, T.L., Tsui, F., Klessig, D.F. and Glazebrook, J. (1998) PAD4 functions upstream from salicylic acid to control defense responses in Arabidopsis. *Plant Cell* 10: 1021–1030.